LONGITUDINAL AND SHEAR WAVE PROPAGATION IN SILICA AEROGELS AT ULTRASONIC FREQUENCIES.

PACS REFERENCE: 43.35.Cg, 43.35.Mr, 43.35.Yb, 43.20.Ks

Gómez Álvarez-Arenas, Tomás E.
Instituto de Acústica del CSIC.
C/Serrano 144, 28006.
Madrid.
Spain
Tel: 915 618 806
Fax: 914 117 651
E-mail: tgomez@ia.cetef.csic.es

ABSTRACT.

In this work, the possibility to use a technique based on the analysis of thickness resonances of air-surrounded aerogel plates at ultrasonic frequencies to obtain its viscoelastic properties is investigated. These resonances were excited and sensed by airborne ultrasonic waves. To this purpose, specially designed air-coupled, high-sensitivity and broad-band piezoelectric transducers were used. Precise and simultaneous measurements of velocity and attenuation of longitudinal and shear waves at different frequencies as well as aerogel density were obtained. It allowed to afford for the first time, a full characterisation of the viscoeleastic properties of these materials at ultrasonic frequencies.

INTRODUCTION.

Aerogels are among the most amazing particulate porous solids. They exhibit unexpected properties: thermal, optical and acoustics. Therefore, these materials have been proposed for many different applications: thermal and acoustic isolation, gas sensors, capacitors, acoustics delay lines, and as acoustic impedance matching layers for air-coupled piezoelectric transducers. Ultrasonics methods have been used to study their properties; while methods to determine ultrasonic longitudinal velocities are well established, attenuation data are limited. Attenuation was measured by Debye-Sears diffraction for the frequency range of 0.8-8 MHz.[1] At lower frequencies (20-200 kHz) a reverberation method was used.[2] There is a lack of experimental results concerning the attenuation of longitudinal waves for the frequency range 0.2-1 MHz and the velocity of shear waves in the aerogel. In addition, to the author's knwoledge, there is nothing at all about attenuation of shear waves.

It is the purpose of this work to apply an air-coupled ultrasonic spectroscopy technique to simultaneously measure sample density and velocity and attenuation of longitudinal and shear ultrasonic waves in aerogel plates. This is possible thanks to the recent developments of air-coupled piezoelectric transducers make possible to produce high-sensitivity and broad-band transducers operating in the frequency range of 0.3-2 MHz.[3, 4, 5] From these results, we achieved a full characterisation of the viscoelastic properties of an aerogel, i.e. to obtain complex-valued and frequency-dependent data for all the elastic constants.

MATERIALS.

The aerogel sample used for this work is a slab (2.4 cm diameter and 0.3 cm height) provided by the Institùt de Ciencia des Materials de Barcelona (CSIC). Details about manufacturing process are given in Ref. 6. Before the measurements the sample was placed in a vacuum chamber and heated to 100 ºC to remove any absorbed moisture

THEORETICAL BACKGROUND.

Generally speaking the technique is as follows: an aerogel plate embedded in a continuum medium (air) is insonificated by a broad-band airborne ultrasonic pulse which frequency spectrum comprises several eigenfrequencies of the plate.[7] Eigenvibrations excited by the incident wave are recorded and analyzed. There are two different theoretical approaches to this problem. The first one is to impose boundary conditions to stress and strains fields at the surfaces of the plate and solve the system of equations for field amplitudes.[8] The second one is to apply the quantum-mechanical theory of resonance scattering.[7] This later procedure calculates the contribution of each resonance to the transmission and reflection coefficients. Exact results are provided only on the vicinity of the resonances but it gives a clear insight on the behaviour of the plate specially in the case of overlapping resonances. In this work the first procedure has been used since overlapping resonances can be discerned. The viscoelastic nature of the plate is introduced into the theoretical analysis by means of the correspondence principle (i.e. introducing complex and frequency dependent elastic constants).[9]

Theoretical modelling of the problem of the transmission of ultrasonic waves through an air surrounded aerogel plate is carried out considering incident plane longitudinal waves. Displacement vector potentials can be written in the three space regions (m) denoted as (1: and 3: air, 2: aerogel plate)

$$\begin{aligned} \boldsymbol{f}_m &= \boldsymbol{f}^{1}_{m}\exp\left[i\boldsymbol{a}_m z\right] + \boldsymbol{f}^{2}_{m}\exp\left[-i\boldsymbol{a}_m z\right] \\ \boldsymbol{j}_m &= \boldsymbol{j}^{1}_{m}\exp\left[i\boldsymbol{b}_m z\right] + \boldsymbol{j}^{2}_{m}\exp\left[-i\boldsymbol{b}_m z\right] \\ \boldsymbol{b}_m &= k_t^m\cos\boldsymbol{q}\,,\quad \boldsymbol{a}_m = k_l^m\cos\boldsymbol{q}\,,\quad m = 1, 2, 3 \end{aligned} \tag{1}$$

where k is the wavenumber in each region (m) of the space, the subscripts l and t denote longitudinal and shear wave respectively, $\boldsymbol{q}$ is the angle of incidence of the acoustic ratiation on the aerogel plate, and t is the thickness of the membrane. Faces of the aerogel are located at $z = 0$ and $z = t$ .Displacement vector u is calculated from the scalar potential $\boldsymbol{j}$ by:

$$u_m = grad\,\boldsymbol{f}_m + rot\,\boldsymbol{j}_m \tag{2}$$

Stress (s) is calculated from the constitutive equations in each region of the space. The aerogel plate can be considered homogeneous and isotropic:

$$\boldsymbol{s}_{ij} = \boldsymbol{l}\frac{\partial u_k}{\partial x_k}\boldsymbol{d}_{\mathrm{ij}} + \boldsymbol{m}\left(\frac{\partial u_i}{\partial u_j} + \frac{\partial u_j}{\partial u_i}\right) \tag{3}$$

where λ and μ are the Lamè coefficients of the aerogel plate. Stress and displacement must be continuous across membrane surfaces ($z = 0$, $z = t$). These boundary conditions along with

Eqs.(1)-(3) provide a linear system of four equations that can be analitically solved for the coefficients j_m^i. From these coefficients, displacements, stress, and energy flux in any point of the space can be derived. The transmission coefficient (*T*) is defined as the ratio of transmitted to incident energy fluxes. For normal incidence (θ=0) a simple analytical expresion for *T* is obtained:

$$T = \frac{4}{2 + 2\cos^2 \tilde{k}_l t + \frac{Z_{aerogel}^4 + Z_{air}^4}{Z_{aerogle}^2 Z_{air}^2} \sin^2 \tilde{k}_l t} \qquad (4)$$

where *t* is the thickness of the aerogel, $\tilde{k}_l = k_l - i\alpha_l = \omega / c_l - i\alpha_l$, where k_l is the wave vector, α_l the longitudinal wave attenuation, c_l the longitudinal phase-velocity, and ω is the angular frequency. *Z* is the specific acoustic impedance. On the contrary, no simple analytical expresion for *T* can be derived for oblique incidence. For this case, a numerical solution is calculated. The employed technique to characterise the aerogel is based on experimental measurement and theoretical calculation of the transmission coefficient of ultrasonic waves through the aerogel plate.

EXPERIMENTAL SET-UP.

For the experimental work two pairs of specially designed air-coupled piezoelectric transducers were used. First, the signal received through the airgap without the membrane in between is digitized by the oscilloscope and transferred to the computer; its frequency spectrum is calculated (Fast Fourier Transform *FFT*). Then the aerogel plate is put in between the transducers, first at normal incidence. The received signal through the airgap and the aerogel plate is again recorded and *FFT* calculated. Finally, the incidence angle is increased and the measurement repeated for several values of the angle of incidence up to 20 degrees.

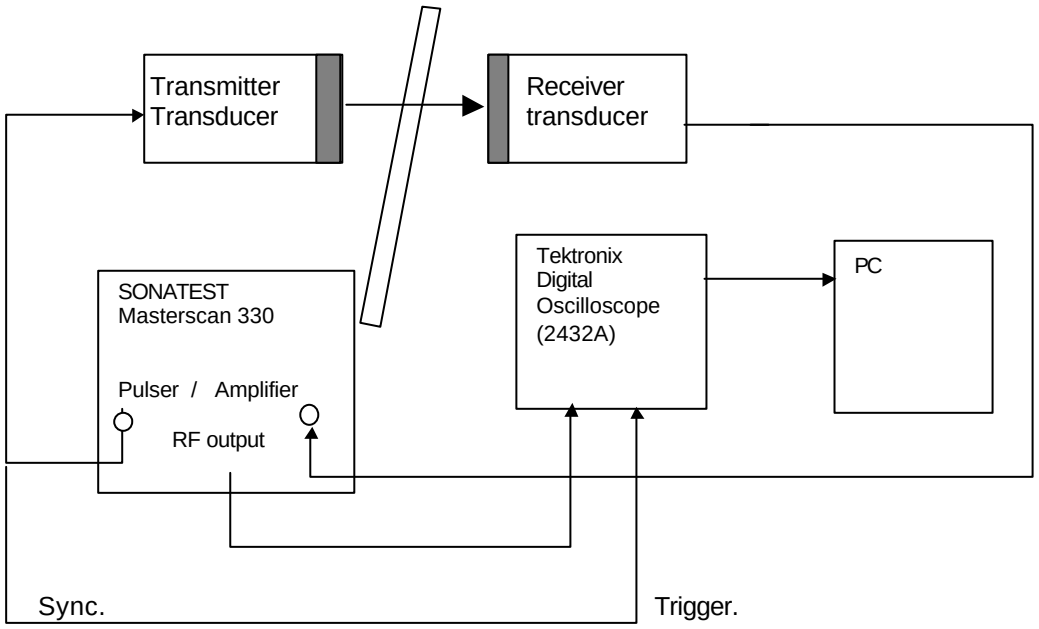

Figure 1. Scheme of the experimental set-up.

The Insertion Loss (*IL*) for the aerogel plate is defined as $IL = 20\log_{10}\left(A_{sample}/A_{ref}\right)$ where A_{sample} and A_{ref} are the amplitudes of the FFT (Fast Fourier Transform) of recorded waves with and without the aerogel plate in between the transducers respectively. In addition, it can be demonstrated that in this case *IL* and *T* follow a simple relation: $A_{sample}/A_{ref} = |T|^{1/2}$.

Figure 1.a. shows the measured *IL* (dots) for normal incidence. Separation between resonances is almost constant and equal to 59±1 kHz. First order resonance might be located at 59 kHz and the first peak in Fig. 1.a (354.5 kHz) should then correspond to the sixth order peak (n=6).

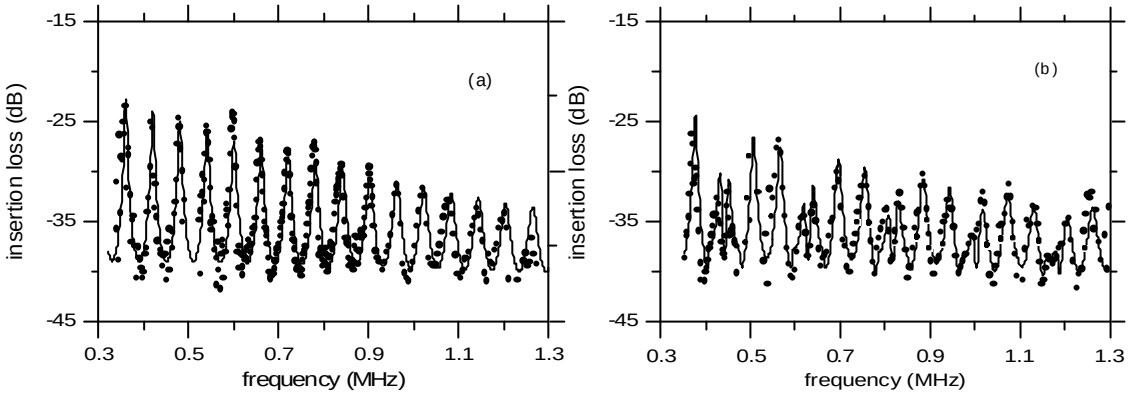

Figure 1. *IL* versus frequency. Dots: experimental measurements. Solid line: theoretical results: 1.a. Normal incidence; 1.b. Incidence angle of : 19º

c_l, α_l, and ρ are used as fitting parameters to match the theoretical calculations of *IL* to the measured values. The result for *IL*, so calculated, is shown in Fig 1.a (solid line). Fig. 2 shows the obtained values of c_l and α_l at resonance. Obtained ρ is 220±20 Kg/m^3. α_l follows a frequency power law:

$$\alpha_l(f) = \alpha_{l_1} f^{y}, \quad \text{where } y = 1.1\pm0.05 \text{ and } \alpha_{l_1} = 3.16\times10^{-5}\, Np/(m.Hz^{y}) \qquad (2)$$

Fig. 1.b shows the measured *IL* (dots) for oblique incidence (19º). Interferences due to the overlap of longitudinal and shear resonances are clearly appreciated. Using the values of c_l and α_l obtained before (analysis of *IL* for normal incidence), shear wave phase-velocity (c_t) and attenuation (α_t) were used as fitting parameters to match theoretical calculations of *IL* to experimental values. The higher accuracy for c_t and α_t are obtained at frequencies were interferences between longitudinal and shear resonances appear. The result for *IL,* so calculated, is shown in Fig 1.b (solid line). Obtained results for c_t and α_t are shown in Fig. 2. For frequencies higher than 0.9 MHz the uncertainty in the determination of α_t becomes very high. Therefore, the error in the determination of the *y* exponent is also very high: *y* = 0.5±0.15. Using thinner samples and/or larger incidence angles might solve this problem. Results for α_t can be adjusted by a power law:

$$\alpha_t(f) = \alpha_{t1} f^{y}, \quad \text{where} \quad y = 0.5,\ \alpha_{t_1} = 0.22\, Np/m/Hz^{0.5} \qquad (3)$$

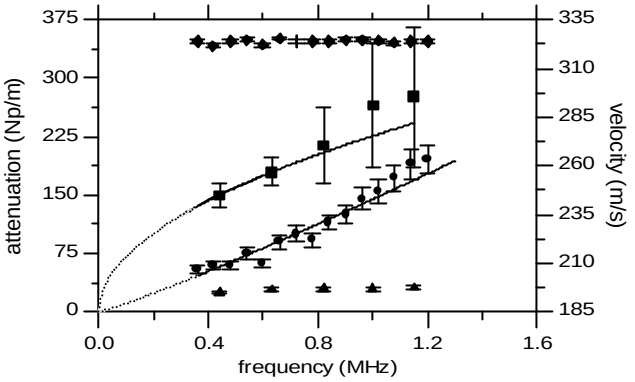

Figure 2. Attenuation versus frequency of longitudinal (•) and shear (■) waves. Solid lines: power fitting. Velocity versus frequency of longitudinal (◆) and shear ( ) waves.

Table I. Poisson coefficient and complex elastic modulus.

Freq. (MHz)	*G* (MPa) Shear Modulus	$\tan^{-1}\delta_G$ = imag(*G*)/real(*G*)	*M* (MPa)	$\tan^{-1}\delta_M$ = imag(*M*)/real(*M*)	*E* (MPa) Young Modulus	$\tan^{-1}\delta_E$ = imag(E)/real(E)
0.44	8.36+0.18i	0.0212	22.98+0.32i	0.0140	20.30+0.38i	0.0185
0.63	8.49+0.15i	0.0179	23.01+0.28i	0.0124	20.53+0.32i	0.0158
0.82	8.54+0.14i	0.0164	23.01+0.31i	0.0132	20.60+0.31i	0.0151
1.0	8.54+0.14i	0.0166	23.16+0.36i	0.0155	20.62+0.33i	0.0162
1.2	8.58+0.13i	0.0151	23.09+0.38i	0.0165	20.67+0.32i	0.0156

Complex elastic constants and related viscoelastic parameters can now be calculated. Results are gathered in table I. The complex shear modulus *G* is obtained from $G = \tilde{c}_t^2 \rho$. The complex elastic modulus *M* is defined as: $M=K+4/3G \equiv \tilde{c}_l^2 \rho$, where *K* is the bulk modulus, and $\tilde{c}_t$ is the complex shear wave velocity. *E* is the Young Modulus: $E = 9GK/(3K+G)$, with real values of the same order as the ones found using microindentation.[10] Poisson coefficient, which is difficult to obtain from other techniques, is calculated from: $\sigma = (2r-1)/2(r-1)$, where $r = c_t^2/c_l^2$.

A detailed analysis of data shown in table I reveals that none of the calculated elastic moduli follow the frequency dependence predicted by any of the simple and basic viscoelastic single relaxation models (Voigt and Maxwell). On the contrary, bearing in mind that attenuation follows a frequency power law (Eqs. 2 and 3), a possible alternative to single relaxation models could be a time causal model. [11, 12]

In some aspects, the behaviour of the aerogel observed here resembles that of some well investigated materials. These similarities permit to gain an insight into the underlying physics. For example, the shear modulus (*G*) and shear loss ($\tan\delta_G$) exhibit a similar behaviour to those reported for some kind of polymers. [11, 13] For such polymers the interpretation usually given is based on non-local cooperative interactions of large molecules which could also be applied for aerogels. Another interesting feature is provided by the fact that $Q_M \equiv \tan^{-1}\delta_M \cong cte \Rightarrow \alpha_l \propto f$. This relationship has also been observed, for some kind of aerogels, at higher and lower frequencies. [1, 2]

A similar behaviour has been found in marine sediments (water-saturated and dry sediments). Theoretical predictions of α_l in fluid-filled porous media (as sediments) are based on the interaction between the fluid in the pores and the solid skeleton. This provides a dependence of the attenuation with the frequency that varies at f^2, f or $f^{1/2}$ depending on the frequency range involved.[14] On the contrary, experimental measurements over a wide frequency range suggest a linear frequency dependence for α_l. This is the object of a long lasting argument between experimentalists and theoreticians.[14] To explain this experimental behavior, different sources of disipation leading to an attenuation proportional to f (e.g. friction at the contact area between particles of the frame) were introduced into the theoretical modeling. The understanding of sound attenuation in aerogels may benefit from this.

CONCLUSIONS.

In conclusion, we present an experimental technique that do not require any sample machining to simultaneously measure velocity and attenuation of longitudinal and shear waves in aerogels. A fully viscoelastic characterisation of the aerogel is obtained and a deeper insight on aerogel basic properties is gained.

REFERENCES.

1. T. Schlief, J. Gross and J. Fricke J. Non-Crys. Solids **145**, 223, (1992).
2. A. Zimmerman, J. Gross and J. Fricke. J. Non-Cryst. Solids **186**, 238 (1995).
3. T.E. Gómez and F. Montero. Bol. Soc. Esp. Cerám. Vidrio **41**(1), 16 (2002).
4. F. Montero, T. E. Gómez, A. Albareda, R. Pérez, J. A. Casals. 2000 IEEE Ultrasonics Symp. Proceedings, 1073, (2000).
5. T. E. Gómez, F. Montero, 2000 IEEE Ultrasonics Symp. Proceedings,1069 (2000).
6. T. E. Gómez, F. Montero, M. Moner-Girona, E. Rodriguez, A. Roig, E. Molins, J.R. Rodríguez, S. Vargas, M. Esteves. 2001 IEEE Ultrasonics Symp Proceedings (Atlanta 7-10), (2001).
7. L. Flax, G. C. Gaunaurd and H. Überall. in *Physical Acoustics vol. XV,* edited by W. P. Mason and R. N. Thurston (Academic Press, 1981).
8. L. M. Brekhovskikh. *Waves in layered media* (Academic Press, New York, 1960)
9. D.R. Bland. *The Theory of linear viscoelasticity* (Pergamon Press, 1960).
10. M. Moner-Girona, A. Roig, E. Molins, E. Martínez and J. Esteve. Appl. Phys. Lett. **75**(5), 653, (1999).
11. T. L. Szabo and J. Wu. J. Acoust. Soc. Am. **107** (5), 2437, (2000).
12. T. L. Szabo. J. Acoust. Soc. Am. **97** (1), 14, (1995).
13. J. D. Ferry. *Viscoelastic properties of polymers* (John Wiley & Sons, 1980).
14. A. C. Kibblewhite. J. Acoust. Soc. Am. **86** (2), 716, (1989).